Applied Innovative Research
Vol. 1, June 2019, pp. 101-105

Template free synthesis of PbS nanoparticles by sol-gel facile method under IR radiation at room temperature

Ravikant, Jyotshana Gaur, Sanjeev K Sharma & Beer Pal Singh*
Department of Physics, Ch Charan Singh University, Meerut 250 004, India

Received 01 June 2019; accepted 19 June 2019

Lead sulfide (PbS) nanoparticles have been synthesized from the precursor of lead nitrite tetrahydrate [$Pb(NO_3)_2.4H_2O$] and thiourea [$CH_4\ N_2S$] at room temperature by sol-gel method under the infrared (IR) irradiation. The synthesized PbS nanoparticles have been characterized by XRD, FE-SEM, UV-vis spectrophotometer, and FTIR. The dominant peak (200) in XRD pattern, microstructure and the absorption of PbS have been confirmed the formation of nanoparticles. The crystallite size of PbS nanoparticle has been observed to be 13 nm. The lattice constant "*a*" of as-synthesized nanostructured PbS powder has been estimated to be 5.99 Å closed to the standard one 5.93 Å. The strain has been determined from W-H Plot and estimated to be 1.75×10^{-3}.

Keywords: PbS nanoparticles, IR radiated Sol-gel synthesis, Microstructural and optical properties

1 Introduction

Lead sulfide (PbS), an important IV-VI semi-conductor material with a direct bandgap has the great interest due to their tunable particle size, optical and electronic properties arising from quantum confinement effect[1-3]. The controlled nanostructured PbS powders and thin films are potentially useful for the various application, for example, IR detectors, solar absorbers, telecommunications, optical switches and amplification, electro-luminescent devices: light emitting diodes (LED), Pb^{2+}ion selective sensors and so on[4-8].

Various synthesis methods have been implemented to synthesize[9] nanostructured PbS powder, that is, polymer templated sol-gel method[10-12], chemical bath deposition[13,14], microwave assisted solution growth[15], hydrothermal[16], chemical vapor deposition[17], physical vapor deposition[18], and IR irradiation chemical bath deposition[19]. Among all synthesis methods, infrared (IR) radiation assisted chemical bath deposition of PbS nanoparticles are fewer synthesized and studied their microstructural and optical properties. Therefore, the synthesis of PbS nanoparticles by using IR irradiation assisted chemical route synthesis method and their microstructure, structural and optical properties are really an informative and contribution towards the scientific community.

*Corresponding author (E-mail: drbeerpal@gmail.com)

2 Experimental: Synthesis and Characterization of PbS Nanoparticles

To synthesize PbS nanoparticles, the precursor of lead nitrite tetrahydrate [$Pb(NO_3)_2.4H_2O$] of 99%, and thiourea [$CH_4\ N_2S$] of 98% were purchased from Sigma-Aldrich of AR grade and used without further purification. 0.2 M the aqueous sol was prepared with deionized (DI) water at room temperature. The reaction was controlled by the magnetic stirrer of mixing drop-by-drop of aqueous solution of thiourea. During the reaction, the IR lamp was illuminated on the solution. Some PbS precipitations were detected during the synthesis process and then filtered by using Whatman filter paper and dried in an Oven.

The microstructure and structural properties of PbS precipitates were determined from scanning electron microscopy (SEM: Carl Zeiss-EBO 18) and X-ray diffraction (XRD: Bruker D8 advance) with CuKα (λ = 1.54 Å) radiation. For elemental compositions, the energy dispersive X-ray spectroscopy (EDAX) were measured in addition of SEM analysis. The optical properties of PbS nanoparticles were determined from UV-visible absorption spectroscopy (Hitachi spectrophotometer, model U-3400). The functional groups were evaluated from FTIR spectrophotometer.

3 Results and Discussion

Figure 1 shows the XRD pattern of PbS nanoparticles ranged 20° - 80° (2θ). The diffraction peaks of PbS nanoparticles were detected at 25.47°,

29.60°, 42.62°, 50.47° and 53.07° corresponding to planes of (111), (200), (210), (311) and (222), respectively. These peaks are indicated to the polycrystalline nature having a cubic lattice structure of the space group of "Fm3m". The dominant and intense peak (200) at 29.60° of PbS nanoparticles showed the crystalline nature. The cubic lattice structure of PbS nanoparticles are consistent with the data of JCPDS (card number 00-001-0880). The crystallite size (D) of PbS Nanoparticles has been calculated using the Scherrer formula[20, 21];

$$D = \frac{0.9\lambda}{\beta \cos\theta} \quad \ldots (1)$$

where λ is the wavelength (λ = 0.154 nm), β is the FWHM of a diffraction peak, θ is the Bragg's angle.

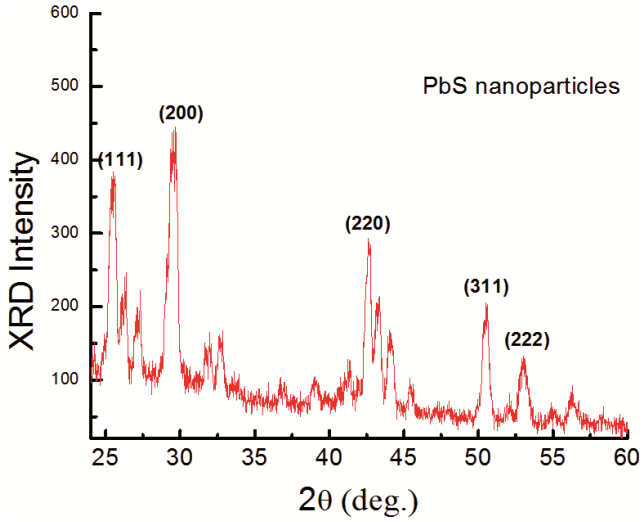

Fig. 1 — XRD pattern of PbS nanoparticles synthesized under IR radiation.

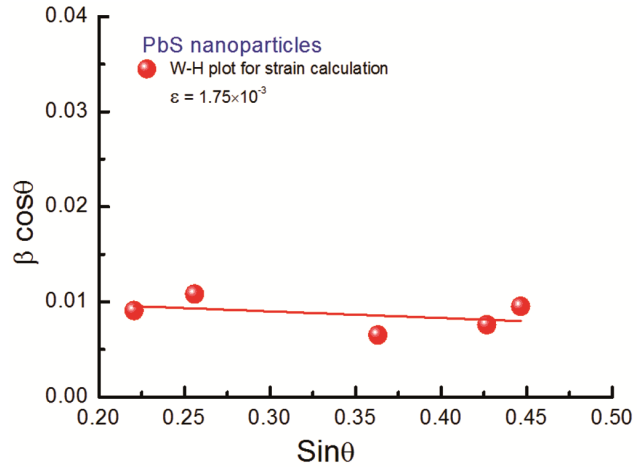

Fig. 2 — W-H plot for strain evaluation of PbS nanoparticles.

The crystallite size of PbS nanoparticle was observed to be 13 nm.

Figure 2 shows the linear fitting of Williamson-Hall (W-H) Plot for nanostructured PbS powder (sinθ versus β cosθ). The crystallite size (D) and internal strain (ε) of as-prepared PbS nanoparticles were obtained by linear fitting of W-H equation[22];

$$\beta_{hkl} \cos\theta = 4\varepsilon \sin\theta + \frac{K\lambda}{D} \quad \ldots (2)$$

where β is the full width at half maximum (FWHM) of the dominant diffraction peak (200), θ is the Bragg's diffraction angle and λ is the wavelength used (λ = 1.54 Å), 'D' is the coherent scattering length (crystallite size) and 'ε' is the internal strain. The strain was determined from W-H Plot and estimated to be 1.75×10^{-3}. The crystallite size (D) is given by intercept of the straight line and using the Williamson-Hall equation. It is well-known that the XRD line broadening was influenced by the crystallite size and the internal strain. The value of 'D' calculated from two different methods are in closed match.

The interplaner distance, d_{hkl}, of as-synthesized PbS nanoparticles can be determined from Bragg's relation;

$$2d_{hkl} \sin\theta = n\lambda \quad \ldots (3)$$

where λ is the wavelength of X-ray radiation source, θ is the Bragg's angle of incidence, and the integer n is the order of the corresponding reflection. The lattice constant "a" of the nanostructured PbS was determined from the XRD peak pattern profiles by using the following formula;

$$d_{hkl} = \frac{a}{\sqrt{h^2 + k^2 + l^2}} \quad \ldots (4)$$

The values of 'd' and 'a' are summarized and given in Table 1. The value of lattice constant "a" of

Table 1 — The lattice constant 'a' is summarized.

S. No.	Plane (hkl)	Peeks angle 2θ (degree)	d_{hkl} (Å)	a (Å)	$a_{average}$ (Å)
1.	(111)	25.48	3.49	6.04	
2.	(200)	29.66	3.00	6.00	
3.	(220)	42.57	2.12	5.99	5.99
4.	(311)	50.502	1.80	5.96	
5.	(222)	53.02	1.72	5.95	

as-synthesized nanostructured PbS powder was estimated to be 5.99 Å, which is in good agreement with the standard value for PbS cubic lattice structure phase of 5.93 Å.

Figure 3 ((a) and (b)) shows the SEM micrographs of polycrystalline PbS nanopowder with two different resolutions marked the scale of 10 μm and 3 μm, respectively. The SEM images showed the morphology of the synthesized PbS Nanoparticles, that is, the mixture of discrete appearance of nanoparticles and an axial growth of small size of nanowires.

Figure 4 shows the EDAX spectrum of as-synthesized nanostructured PbS powder. The elemental analysis of PbS was confirmed the Pb and S along with other impurity oxygen peak (O), which might be occurred due to the adsorption of oxygen

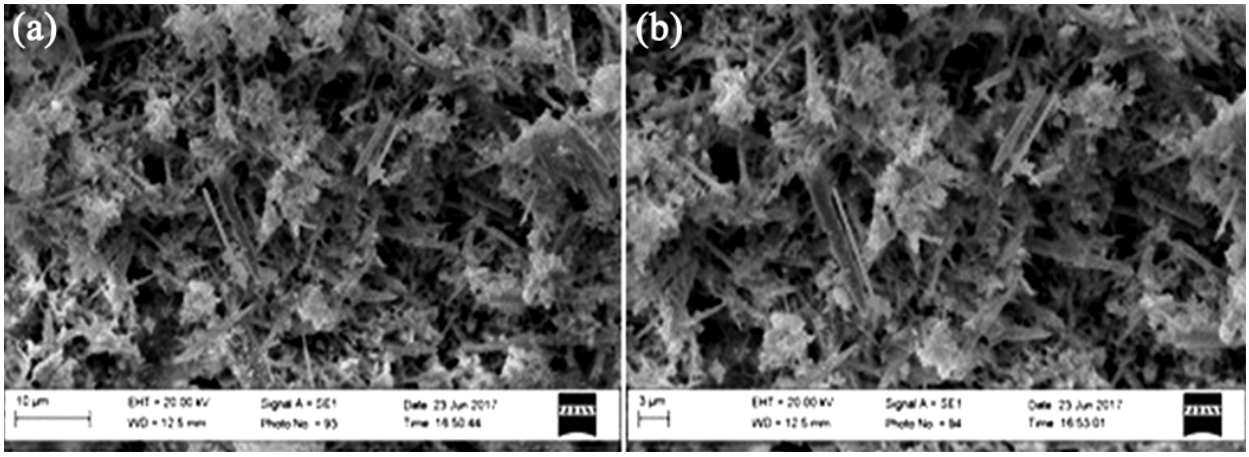

Fig. 3 — SEM micrographs of nanostructured PbS powder synthesized under IR radiation.

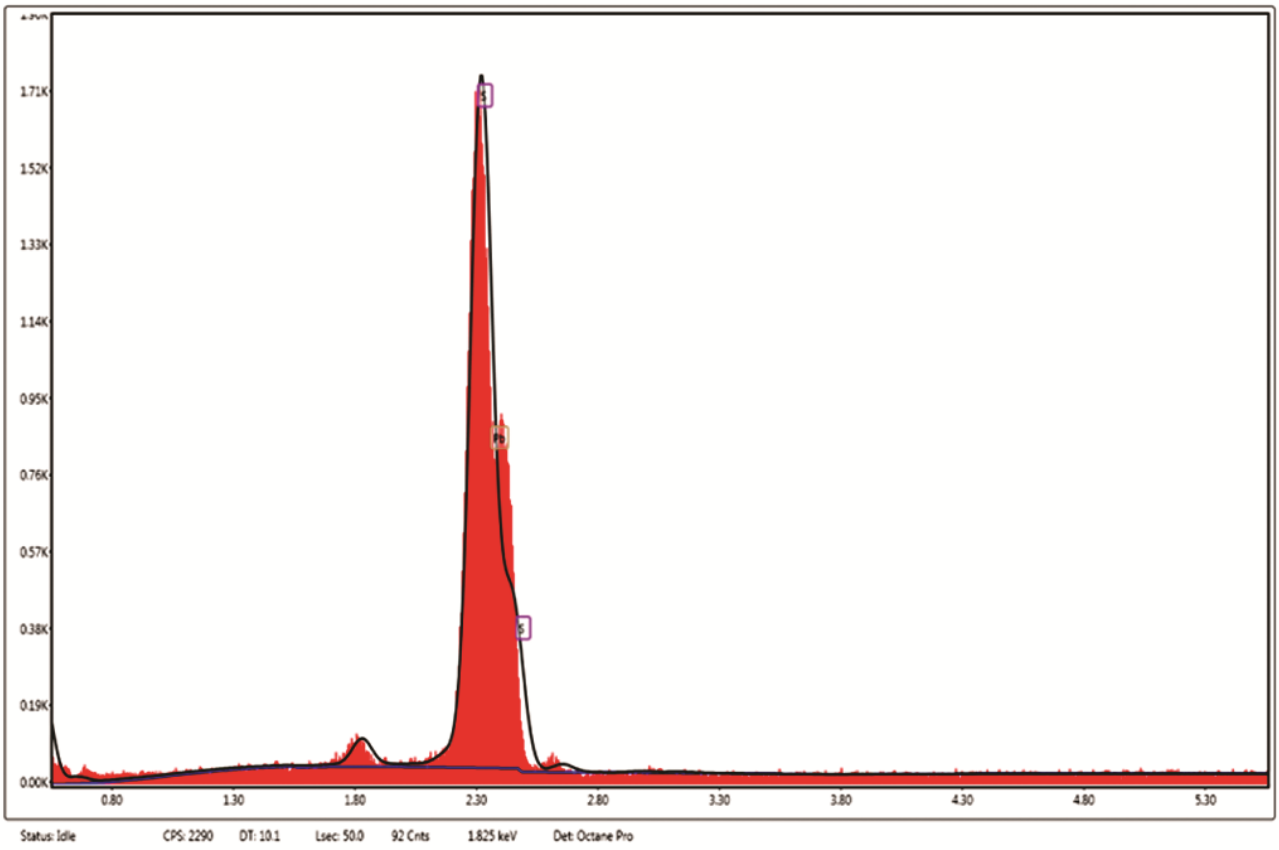

Fig. 4 — EDAX spectrum of as-synthesized PbS nanoparticles.

from atmosphere during the measurement of reacted at the surfaces of nanoparticles. The elemental composition of PbS is summarized in Table 2.

Figure 5 shows the UV-Vis absorption spectrum of as-synthesized nanostructured PbS nanoparticles. The bandgap of nanostructured PbS was calculated from Tauc's plot[23] and observed to be 4.27 eV, which was observed to the reported one for nanoparticles[16].

Figure 6 shows the FTIR spectrum of nanostructured PbS powder recorded in the range of 750 - 4000 cm^{-1} at room temperature. This spectrum indicated the presence of organic species at surfaces of nanoparticles, which

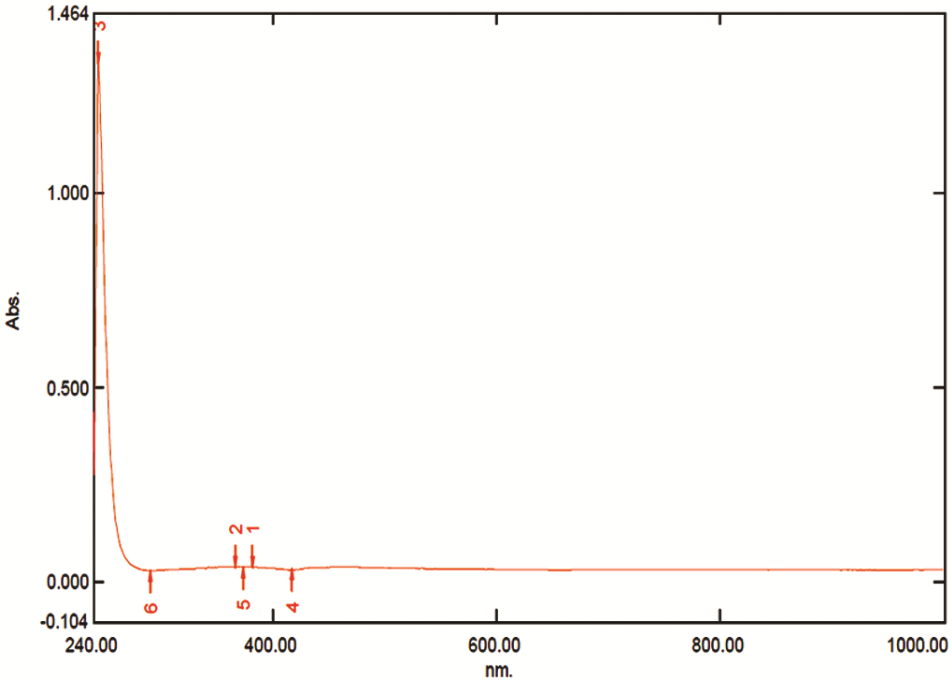

Fig. 5 — UV-Vis spectroscopy of as-synthesized PbS nanoparticles.

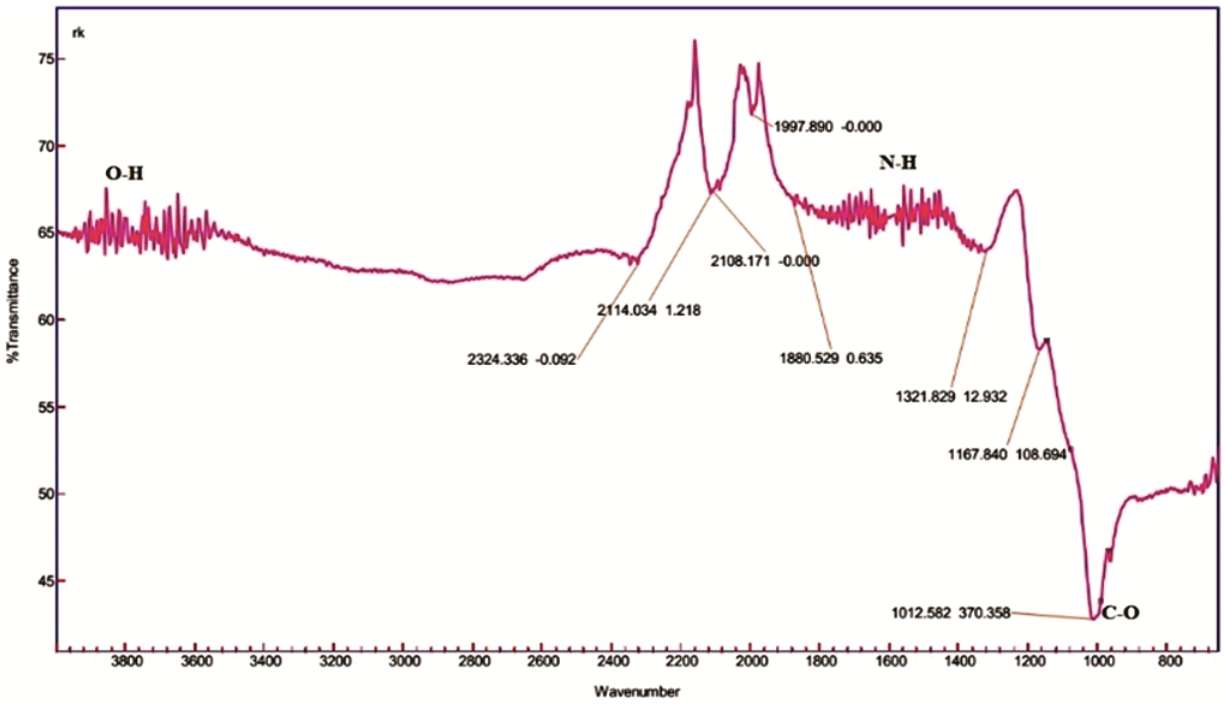

Fig. 6 — FTIR spectrum of nanostructured PbS powder synthesized under IR radiation.

Table 2 — The Elemental ratio of as-synthesized PbS nanoparticles

Element	Weight%	Atomic%
S K	27.12	21.33
Pb M	28.20	3.61
O K	44.68	75.05
Totals	100	100

identifying the chemical nature of surface compounds. The FTIR also showed the bonding structure and orientation of the adsorbed entity. As per the analysis of Hardinger's Five Zone Analysis, we identified the presence of bonding O-H, C-O and N-H at the spectral data[16]. At the lower wave number, it is confirmed the presence of hetero polar diatomic of lead sulfide molecules[24].

4 Conclusions

Nanostructured PbS powder is synthesized from IR irradiated CBD method successfully. The XRD pattern of nanostructured PbS showed the polycrystalline nature of the powder. The mixture of discrete appearance of nanoparticles and an axial growth of small size of nanowires were detected in SEM micrographs. While the stoichiometric ratio of Pb and S in the nanostructured PbS were detected in EDAX spectrum. The broadening of peaks indicated that particles are in nanometer range (13 nm) and are in good agreement with SEM images. The strain was determined from W-H Plot and estimated to be 1.75×10^{-3}. The bandgap of nanostructured PbS was evaluated from Tauc's plot to be 4.27 eV. The FTIR spectral data showed the O-H, C-O and N-H bands at lower wavenumber, which confirmed the presence of PbS molecule.

Acknowledgement

The funding for this research work was supported from DST-FIST sponsored project SR/FST/PSI-177/2012.

References

1 Kanazawa H & Adachi S, *J Appl Phys*, 83 (1998) 5997.
2 Dantas N O, Paula P M N D, Silva R S, López-Richard V & Marques G E, *J Appl Phys*, 109 (2011) 024308.
3 Greben M, Fucikova A & Valenta J, *J Appl Phys*, 117 (2015) 144306.
4 Ullrich B, Xi H & Wang J S, *J Appl Phys*, 115 (2014) 233503.
5 Yousefi R, Mahmoudian M R, Sa´aedi A, Cheraghizade M, Jamali-Sheini F & Azarang M, *Ceram Int*, 42 (2016) 15209.
6 Al-Zuhery A M, Al-Jawad S M & Al-Mousoi A K, *Optik*, 130 (2017) 666.
7 Göde F & Ünlü S, *Mater Sci Semicond Process*, 90 (2019) 92.
8 Priyanka U, Akshay G K M, Elisha M G, Surya T B, Nitish N & Raj M B, *Int Biodeterior Biodegr*, 119 (2017) 78.
9 Soetedjo H, Siswanto B, Aziz I & Sudjatmoko, *Res Phys*, 8 (2018) 903.
10 Mamiyev Z Q & Balayeva N O, *Opt Mater*, 46 (2015) 522.
11 Nejo A O, Nejo A A, Pullabhotla R V S R & Revaprasadu N, *J Alloys Compd*, 537 (2012) 19.
12 Li M, Yang Y, Yuan X, Liu Y & Zhang L, *Mater Lett*, 149 (2015) 62.
13 Yücel E & Yücel Y, *Ceram Int*, 43 (2017) 407.
14 Joshi R K, Kanjilal A & Sehgal H K, *Appl Surf Sci*, 221 (2004) 43.
15 Onwudiwe D C, *Heliyon*, 5 (2019) e01413.
16 Davar F, Mohammadikish M, Loghman-Estarki M R & Masteri-Farahani M, *Ceram Int*, 40 (2014) 8143.
17 Yousefi R, Cheraghizade M, Jamali-Sheini F, Basirun W J & Huang N M, *Curr Appl Phys*, 14 (2014) 1031.
18 Beatriceveena T V, Prabhu E, Jayaraman V & Gnanasekar K I, *Mater Lett*, 238 (2019) 324.
19 Singh B P, Upadhyay R K, Kumar R, Yadav K & Areizaga-Martinez H I, *Adv Opt Technol*, 2016 (2016) 6.
20 Kaur N, Sharma S K, Kim D Y & Singh N, *Physica B: Condensed Matter*, 500 (2016) 179.
21 Sharma H K, Archana R, Sankarganesh R, Singh B P, Ponnusamy S, Hayakawa Y, Muthamizhchelvan C, Raji P, Kim D Y & Sharma S K, *Solid State Sci*, 94 (2019) 45.
22 Seetharaman A & Dhanuskodi S, *Spectrochim Acta Part A*, 127 (2014) 543.
23 Sharma S K, Baveja J & Mehra R M, *Physica Status Solidi A*, 194 (2002) 216.
24 Pentia E, Pintilie L, Matei I, Botila T & Pintilie I, *Inf Phys Technol*, 44 (2003) 207.